Towards treatment of liver fibrosis: Cells, targets and models

Helm, D. van der

CHAPTER 5

5

Local and systemic elevated Cripto levels during liver fibrogenesis

Danny van der Helm*, Sofia Karkampouna*, Arwin Groenewoud, Ewa B. Snaar-Jagalska, Bart van Hoek, Hein W. Verspaget, Marianna Kruithof-de Julio#, Minneke J. Coenraad#

*These authors contributed equally to this work

#Joint senior authorship

Abstract

Background

CRIPTO-1 is an (onco)foetal protein that is silenced postnatally and often re-expressed in neoplastic processes. Cell survival and cell proliferation are some of the processes stimulated by CRIPTO-1, which are also known to be important during liver regeneration and fibrogenesis. In the present study we assessed whether CRIPTO-1 is (re-)expressed during liver fibrogenesis.

Methods

Liver tissues of patients with cirrhosis and of experimental liver fibrosis in zebrafish embryos and mice, induced with thioacetamide or carbon tetrachloride, respectively, were evaluated for CRIPTO-1 expression. Immuno-histochemical staining and qPCR for collagen, α-SMA and CRIPTO-1 were performed to determine their expression levels. In addition, CRIPTO-1 levels were assessed in pre- and post-liver transplantation (LT) plasma samples of patients treated for end-stage liver cirrhosis.

Results

CRIPTO-1 was expressed in hepatocytes of humans, zebrafish embryos and mice during fibrogenesis. In humans, CRIPTO-1 expression was positively correlated with the MELD score for end-stage liver disease. Furthermore, patients with end-stage liver cirrhosis showed elevated CRIPTO-1 levels in plasma, which had decreased one year after LT.

Conclusion

Multiple species show enhanced CRIPTO-1 during fibrogenesis and elevated CRIPTO-1 plasma levels in humans with cirrhosis normalize after LT. Altogether, these results are indicative for a functional role of CRIPTO-1 in fibrogenesis which warrant further mechanistic studies.

Introduction

CRIPTO-1 (Teratocarcinoma-Derived Growth Factor 1; TGDF1) is a GPI-anchored signalling protein and member of the epidermal growth factor-CRIPTO/frl/cryptic (EGF-CFC) family, with diverse functions in embryogenesis and as regulator of stemness[1-3]. CRIPTO-1 is silenced postnatally and often re-expressed in neoplasms of breast, lung, prostate, ovarian, bladder, colon, skin, and brain, were it is thought to be involved in cancer progression and metastasis[2,4-12]. Recently, CRIPTO-1 expression was found to be associated with poor overall survival and faster tumour recurrence in patients with hepatocellular carcinoma (HCC), but the underlying mechanism(s) are still largely unknown[3,13]. Suggested mechanisms include CRIPTO-1 involvement in both the classical canonical and the non-canonical signalling pathways, leading to faster proliferation and onset of epithelial to mesenchymal transition of tumour cells[3,14]. Previous research of our group showed that HCCs with high CRIPTO-1 expression show a poorer response to Sorafenib, an oral multi-kinase inhibitor[14,15]. Furthermore, we observed in an experimental model that administration of CRIPTO-1 inhibitors sensitize HCCs for Sorafenib treatment[14].

HCC mostly evolve in a background of cirrhosis, which may be caused by chronic exposure of the liver to damaging factors such as alcohol and viral hepatitis B or C (HBV, HCV)[16]. These factors may lead to damaged and apoptotic hepatocytes, which are thought to activate stellate cells. Subsequently, stellate cells differentiate into myofibroblasts and produce excessive amounts of extracellular matrix components (ECM) as observed in fibrogenesis[17-19]. Chronic fibrogenesis leads to fibrosis, cirrhosis and eventually increases the risk of HCC development. This pathophysiological mechanism and course of the disease are highly conserved between species including human, rat, mouse and zebrafish[17,20,21].

Fibrosis, cirrhosis and HCC are major health problems, HCC being the third most frequent cause of cancer-related death, with a lack of effective antifibrotic treatment options[22-24]. Withdrawal of the injuring stimulus is the only current treatment for liver fibrosis, which in some cases leads to the resolution of fibrogenesis[25]. For end-stage liver cirrhosis, liver transplantation (LT) is still the only curative treatment option of which feasibility depends on patient condition and donor availability, but LT is still a major surgical intervention with substantial risks[26-28]. Therefore, therapies directly targeting fibrogenesis are needed. Better understanding of the pathological mechanisms underlying the fibrosis-cirrhosis–HCC disease cascade could lead to identification of new biomarkers to monitor the disease and may also lead to new targets for the development of alternative treatment strategies.

CRIPTO-1 is a cancer stem cell marker known to maintain stemness as well as to support cell survival and cell proliferation[3,15]. These latter processes are also important during fibrogenesis, regeneration and repair of liver tissue[29-31]. In a previous study, we showed CRIPTO-1 to be highly expressed in HCC and associated with resistance to Sorafenib treatment. Coincidentally,

we observed a relatively high CRIPTO-1 expression in a majority of the cirrhotic liver tissues[14]. Given that CRIPTO-1 is not expressed in liver tissue of healthy adults, we wondered what this CRIPTO-1 re-expression implies for the fibrogenic cascade in the liver. Therefore, in the present study we assessed whether CRIPTO-1 is expressed during liver fibrogenesis in different species and whether this was related with the severity of the disease. CRIPTO-1 expression was evaluated in liver tissue of humans with cirrhosis and in validated zebrafish embryo- and mouse-models for liver fibrogenesis. Furthermore, we also assessed whether enhanced liver CRIPTO-1 was reflected in circulating blood levels of patients with cirrhosis and whether these levels were affected by removing the fibrogenic liver by LT. CRIPTO-1 expression in different species and a correlation with disease stage, could imply a functional role for CRIPTO-1 in the fibrosis–cirrhosis-HCC cascade rendering it a potential interesting marker for disease monitoring or even as a treatment target.

Material and Methods

Patients and controls

All experiments with human specimens were approved by the ethical research committee of the Leiden University Medical Center (LUMC, protocol number: B15.006). Materials were used in compliance with the rules prescribed by the regulations of the LUMC Liver diseases Biobank and with a signed informed consent of the donors. CRIPTO-1 plasma levels were measured in paired pre- and post-LT plasma samples from patients with alcoholic liver disease (ALD, N=25) or viral hepatitis (N=20) related cirrhosis, with plasma from healthy volunteers (N=16) as controls. Post-LT samples were collected and stored at 1 year after LT. Exclusion criteria for this study were the presence of HCC, a combined etiology of cirrhosis, death or re-LT within one year after LT and the development of serious adverse events after LT, such as Tacrolimus induced renal insufficiency (Table 1: patient characteristics). For mRNA-qPCR and (immuno)-histochemical analysis, control tissue (N=5) and alcohol- or viral hepatitis-induced fibrotic/cirrhotic liver tissue (N=19) were obtained from the tissue collections of the LUMC Liver diseases Biobank and Pathology department. These tissues were not from the same patients from which the above mentioned plasma samples were available. The liver tissues were obtained during LT, resection of colorectal cancer-derived liver metastasis, or HCC resection. Clinical data were extracted from the database, including laboratory assessments and clinical MELD (Model for End-Stage Liver Disease) scores, a scoring system for assessing liver function impairment in cirrhosis and risk of short-term mortality.

Table 1: Patient characteristics. Data presented as median (range) for continuous variables and percentage (number) for categorized variables.

Variable	Healthy controls (N=16)	Pre-LT (N=45)	Post-LT (N=45)
Gender (male), % (n)	50% (8)	78% (35)	
Age (median, range)	29 (23-65)	54 (42-69)	
Aetiology			
Alcoholic liver disease		25	
Viral Hepatitis		20	
Blood (median, range)			
AST (U/L)		72 (24-517)	27 (11-240)
ALT (U/L)		37 (15-360)	25 (8-401)
INR		1.2 (1-2.4)	1.0 (0.9-2.4)
ALP (U/L)		130 (50-555)	88 (47-487)
Creatinin (µmol/L)		92 (34-171)	111 (68-204)
γGT (U/L)		43 (7-374)	39 (9-1395)
Sodium (mmol/L)		138 (124-156)	142 (134-148)
Bilirubin (µmol/L)		46 (5-593)	12 (5-29)
Platelet count (10^9/L)		72 (30-142)	144 (93-243)
CRIPTO-1 plasma (pg/ml)	0 (0-818)	1381 (0-12108)	357 (0-5314)
Clinical scores			
MELD		15 (8-33)	10 (6-18)

LT = Liver Transplantation, ALD = Alcoholic Liver Disease, AST = Aspartate aminotransferase, ALT = Alanine aminotransferase, INR = International Normalized Ratio, ALP = Alkaline phosphatase, γGT: gamma-glutamyltransferase, MELD = Model for End-Stage Liver Disease

Mouse and zebrafish embryo models for liver fibrosis

All animal experiments were performed in compliance with the guidelines for animal care and approved by the LUMC Animal Care Committee. Mice received food and water *ad libitum* and were housed under 12h day/night cycle. Liver fibrosis was induced in 6 week old male C57Bl/6Jico mice (Charles River Laboratories, The Netherlands) as described previously[32]. For a period of 11 weeks, mice received 2 intraperitoneal injections per week with carbon tetrachloride (CCL4) in mineral oil (Sigma-Aldrich Chemie BV, Zwijndrecht, The Netherlands). The first week, mice received 2 initiating higher dosages of CCL4 of 1 ml/kg. The following 10 weeks a maintenance dose of 0.75 ml/kg was given twice weekly. At the end of 11th week, mice were sacrificed and livers collected and subsequently fixated with 4% paraformaldehyde for paraffin embedding and stored in isobutyl for RNA isolation.

Liver-fatty-acid-binding-protein (LFABP)-GFP zebrafish embryos were used for the induction of fibrosis with thioacetamide (TAA) as previous described by our group[21,33]. In short, 2 days post fertilisation (dpf) old zebrafish embryos were maintained for 6 days in egg water (water with 60 µg/ml instant ocean, sea salt) supplemented with 0.06% TAA (Sigma-Aldrich Chemie

BV, Zwijndrecht, The Netherlands). After the induction of fibrosis, the embryos were collected and stored in PAXgene blood RNA solution (PreAnalytiX, Hombrechtikon, Switzerland) for RNA isolation.

Histological examination of fibrosis

To evaluate the severity of fibrosis in human and mouse liver tissue, a Sirius-red staining was performed to visualize the amount of collagen deposition. Paraffin sections (4 µm) were hydrated and subsequently stained for 90 min with 1 g/L Sirius-red F3B in saturated picric acid (both Klinipath). Next, the sections were incubated for 10 min with 0.01 M HCL, dehydrated and mounted with Entellan (Merck KGaA, Darmstadt, Germany). Fixed microscope settings were used to capture 5-8 representative images (10x magnifications) which were subsequently used to quantify the amount of staining with ImageJ software (ImageJ 1.47v, National Institutes of Health, USA). With fixed treshold settings, based on control tissues, positive pixels were measured and the respective percentage to the total image calculated and defined as the positive area.

Immuno-histochemical staining, imaging and quantification

Immuno-histochemical stainings were performed to evaluate the expression of CRIPTO-1 and α-smooth muscle actin (α-SMA) in fibrotic and control human and mouse liver tissue. Paraffin tissue sections (4 µm) were hydrated and endogenous peroxidases blocked with 0.3% H_2O_2/methanol (20 min). Antigen retrieval was performed by 10 min boiling in citrate buffer (0.1 M, pH 6.0). After cooling down, primary antibodies detecting mouse- and human-CRIPTO-1 (both kindly provided by Dr Gray Clayton Foundation Laboratories for Peptide Biology, The Salk Institute for Biological Studies, La Jolla, California, USA) and anti-α-SMA (A2547, clone 1A4; Sigma, Buchs, Switzerland) were added and incubated overnight. Next day, mouse- and human-CRIPTO-1 staining was visualised with Alexa fluor 647 secondary antibody and mouse-α-SMA staining with Alexa fluor 488 secondary antibody. In addition a nuclei DAPI staining was performed (Sigma). Representative pictures were captured using a confocal microscope (Leica Biosystems BV, Amsterdam, The Netherlands) and 40x 1.4NA oil-immersion objective with fixed microscope and software settings. Human-α-SMA staining was visualised by 1h incubation with a secondary goat anti-rabbit-HRP conjugated antibody followed by a 10 min incubation with 3,3'-diaminobenzidine (DAB Fast Tablet, Sigma-Aldrich, St. Louis, MO). Nuclear counterstaining was performed with hematoxylin after which the sections were dehydrated and mounted with Entellan. Subsequently, 5-10 representative pictures were captured and used for quantification. The amount of DAB or fluorescent staining in the representative pictures was quantified with ImageJ software. For the CRIPTO-1 staining, the positive area was measured with fixed treshold settings, based on control tissues, and defined as a percentage of positive pixels compared to the total pixels within the hepatocyte regions, regions such as the vessels, bile ducts and the septa with ECM were excluded from the analysis. For the α-SMA stainings, whole images were used to quantify the positive area.

RNA isolation, cDNA synthesis and quantitative Polymerase Chain Reaction (qPCR)

Mouse and human liver tissues were homogenised with UltraTurrax homogenizer (T25 basic, IKA) and TRIpure reagent (Roche). Subsequently, mRNA was isolated following TRIpure RNA isolation protocol. Per experiment, 20 zebrafish embryos were pooled and homogenised by 48h incubation with PAXgene Blood RNA solution at 4°C and next RNA was isolated with NucleoSpin RNA kit (Machery-Nagel GmbH, Düren, Germany). Promega standard protocol was used to synthesise cDNA from 1 µg RNA (Promega, Madison, Wisconsin, USA). CRIPTO-1, collagen-1α1 and α-SMA expression in human and mouse samples and CRIPTO-1, collagen-1α1 and Acta-2 expression in zebrafish embryos samples were measured by qPCR analysis. QPCR reaction mixtures consisted of 5 µl iQ SYBR Green supermix reagent (Bio-Rad Laboratories, Berkeley, California, USA, 1708886), 1 nM primers and 4 µl cDNA. Results were normalised to β-actin for mouse and human samples and to ribosomal protection protein for zebrafish embryo samples (Supplemental table 1: primer sequences).

Plasma CRIPTO-1 measurements

CRIPTO-1 levels in plasma were measured using ELISA, performed according to manufacturer's protocol (R&D systems, Minneapolis, Canada, DY145).

Statistical Analysis

IBM SPSS statistics software (SPSS Inc. Chicago, IL USA, version 23) was used to perform Spearman tests for correlations. GraphPad Prism software (GraphPad Software, version 5.01, San Diego, CA) was used to perform Student's t-test for the comparison between 2 groups. P-values lower than 0.05 were considered to be statistically significant. The data in the graphs are presented as means ± standard error of the mean (SEM).

Results

CRIPTO-1 expression in patients with end-stage liver cirrhosis correlates with the laboratory MELD score

The presence of liver fibrosis was evaluated by Sirius-red stained collagen-1α1 deposition and α-SMA stained activated stellate cells. Liver tissue of patients with cirrhosis showed significantly more Sirius-red and α-SMA staining compared to control tissue (which validated the clinical indication of cirrhosis, Figure 1A and B). CRIPTO-1 expression in these tissues was mainly observed in the hepatocytes and was clearly more present in the cirrhotic tissue as compared to control tissue, with 16 out 19 (84.2%) cirrhotic livers above the highest level in control livers (Figure 1A and B). Furthermore, the results showed a positive correlation between the amount of CRIPTO-1 staining and the laboratory MELD scores of the patients (correlation coefficient: 0.577, $P<0.003$). No significant correlations between the CRIPTO-1

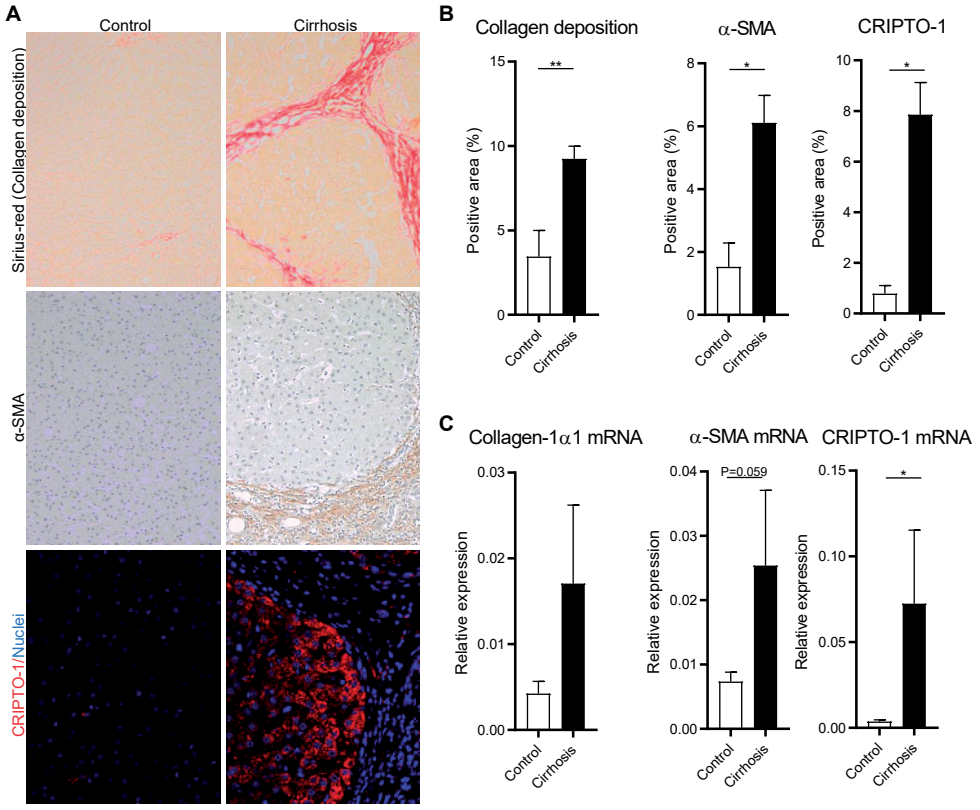

Figure 1. CRIPTO-1 expression in patients with end-stage liver cirrhosis. Liver tissue samples of patients with ALD or viral induced liver cirrhosis (N=19) and controls (N=5) were randomly selected to evaluate CRIPTO-1 expression. (A) Representative pictures of control and cirrhotic liver tissue stained for collagen deposition (Sirius-Red), α-SMA and CRIPTO-1 (CRIPTO-1 in Red, Nuclei in Blue, 100x magnifications). (B) Quantification of Sirius-red, α-SMA and CRIPTO-1 staining (mean±SEM). (C) mRNA expression levels of collagen-1α1, α-SMA and CRIPTO-1 normalized to β-actin (mean±SEM). *p≤0.05 **p≤0.01

and Sirius-red or α-SMA staining were observed (data not shown). QPCR analysis also showed elevated collagen-1α1, α-SMA and CRIPTO-1 mRNA expression levels in cirrhotic liver tissue compared to control liver tissue (Figure 1C). Altogether, these results indicate that livers of patients with cirrhosis express higher levels of CRIPTO-1 compared to control liver tissue and that the amount of CRIPTO-1 staining is correlated to the MELD score.

CRIPTO-1 expression is upregulated in liver tissue of mice and zebrafish embryos with chemically-induced fibrosis

To study whether expression of CRIPTO-1 in liver fibrogenesis also occurs in other species, we evaluated CRIPTO-1 expression in two *in vivo* models: a CCL4 induced mouse model for liver fibrosis and in our recently described TAA-induced zebrafish embryo model for liver fibrosis. In the mouse model, liver fibrosis was confirmed by Sirius-red and α-SMA staining

of the paraffin embedded liver tissue (Figure 2A). Quantification of the Sirius-red and α-SMA staining revealed more collagen deposition and activated stellate cells in the livers of mice with fibrosis compared to healthy control animals (Figure 2B). Similar as observed in humans (Figure 1), CRIPTO-1 staining was more pronounced in the liver tissues of mice with fibrosis and mainly observed in the hepatocytes (Figure 2A and B). These findings were further supported by qPCR analysis, which also showed higher collagen-1α1, α-SMA and CRIPTO-1 mRNA expression in the livers of mice with liver fibrosis compared to the healthy control livers (Figure 2C).

In addition, we evaluated CRIPTO-1 expression in our TAA-induced zebrafish embryo model for liver fibrosis[21]. QPCR measurements showed increased expression levels of collagen-1α1 and Acta-2 (the zebrafish homologue for α-SMA) after TAA treatment which indicates the onset of liver fibrogenesis (Figure 3). In this model, CRIPTO-1 mRNA expression was also higher in embryos with liver fibrosis as compared to healthy control embryos (Figure 3). Thus, both

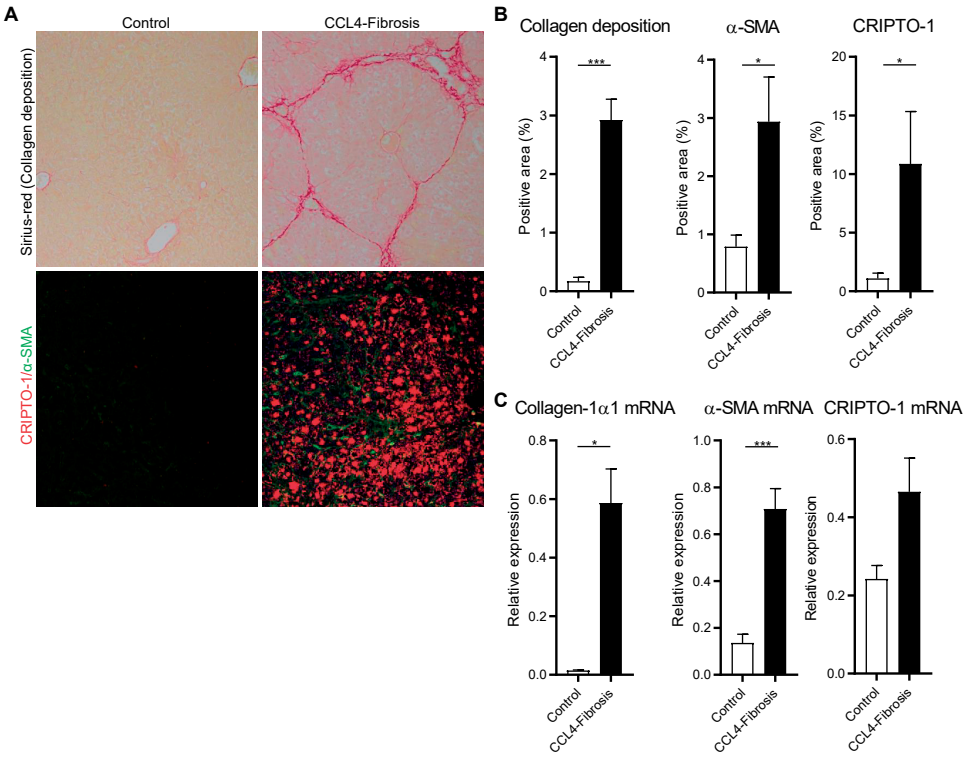

Figure 2. CRIPTO-1 is upregulated in a CCL4 based mouse model for liver fibrogenesis. Mice received chronic administration of CCL4 to induce liver fibrosis. (A) Representative pictures of healthy control and fibrogenic liver tissue stained for collagen deposition (Sirius-Red) or duo-stained for α-SMA (green) and CRIPTO-1 (red) (100x magnifications). (B) Quantification of Sirius-Red, α-SMA and CRIPTO-1 staining (N=8 mice, mean±SEM). (C) mRNA expression levels of collagen-1α1, α-SMA and CRIPTO-1 normalized to β-actin (N=8 mice, mean±SEM). *p≤0.05 ***p≤0.001

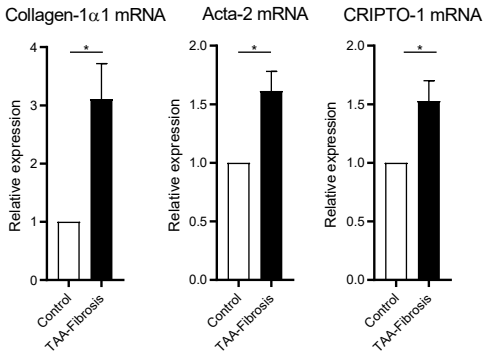

Figure 3. Elevated CRIPTO-1 levels in a zebrafish embryo model for liver fibrogenesis. Collagen-1α1, Acta-2 and CRIPTO-1 mRNA levels normalised to ribosomal protection protein in control zebrafish embryos and embryos with TAA-induced fibrosis. The graphs represent values of three independent experiments (mean±SEM). *p≤0.05

in vivo models show similar results as observed in the experiments with human materials where CRIPTO-1 expression was higher in livers of patients with cirrhosis.

CRIPTO-1 level in plasma decreases after liver transplantation

ELISAs were performed to study whether CRIPTO-1 is reflected in blood of patients with liver cirrhosis. CRIPTO-1 was detected in 31 out of 45 plasma samples of patients with end-stage cirrhosis and only in 2 out of the 16 controls (Chi-square 15.1; p<0.001). The mean CRIPTO-1 level in these detectable samples (3070 pg/ml) was significantly (P=0.03) higher in the end-stage liver cirrhosis group compared to that of the healthy controls (653 pg/ml). In this sub-cohort, the laboratory MELD scores did not correlate with the CRIPTO-1 levels in the blood (correlation coefficient: 0.151, P=0.310).

One year after LT, CRIPTO-1 levels had decreased in all 31 patients as compared to their initial level before transplantation (Figure 4). Furthermore, on average a significant decrease of CRIPTO-1 in post- versus pre-LT plasma samples was observed (Table 1, Figure 4). A significant decrease in plasma CRIPTO-1 was also observed when the ALD and viral-induced cirrhosis cohorts were analysed separately (Supplemental Figure 1A and B). Altogether these data indicate that CRIPTO-1 level in plasma decreases significantly once the cirrhotic liver has been replaced by a healthy donor liver. The mean post-LT plasma level of CRIPTO-1 (1044 pg/ml) did not differ (P=0.6) from the healthy controls (653 pg/mL). However, the frequency of detectable CRIPTO-1 levels between these groups was very different (27/31 for patients versus 2/16 for controls, Chi-square 24.9; p<0.0001).

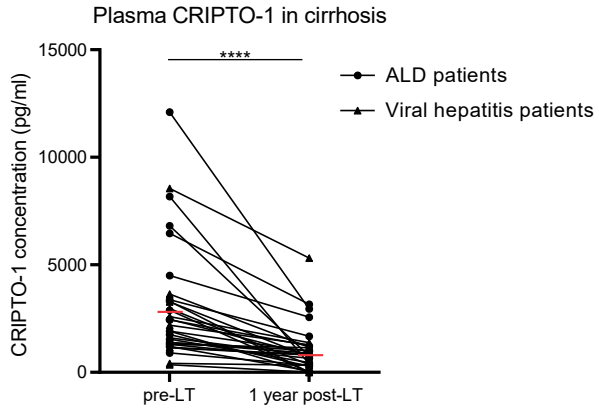

Figure 4. CRIPTO-1 levels in plasma decrease after liver transplantation. CRIPTO-1 levels in and pre- and post-LT paired plasma samples of patients suffering from ALD or viral induced cirrhosis (N=31). Mean group levels are indicated by a red line. ***p≤0.001

Discussion

Liver fibrosis, cirrhosis and hepatocellular carcinoma are major health problems, and treatments which specifically targeting fibrogenesis and thereby preventing progression of the disease are still not available[22-24]. Identification of novel biomarkers in the fibrosis-cirrhosis-HCC cascade could lead to improved monitoring of the course of the disease or even provide alternative targets of treatment. In the present study, we assessed whether CRIPTO-1 is expressed in liver tissue of humans, mice and zebrafish embryos during fibrogenesis. We found that CRIPTO-1 is expressed in hepatocytes of patients with liver cirrhosis and that these expression levels positively correlate with the MELD scoring system for end-stage liver diseases[34,35]. In mouse- and zebrafish embryo-models for liver fibrosis, we observed the same phenomenon, indicative for a general and well preserved role of CRIPTO-1 during fibrogenesis. In addition, we observed elevated CRIPTO-1 levels in the plasma of patients with end-stage liver disease, as a reflection of the liver CRIPTO-1 accumulation, which decreased 1 year after orthotopic liver transplantation.

The observed CRIPTO-1 expression in hepatocytes of human cirrhotic liver tissue is in line with the findings of our previous HCC study where we showed that CRIPTO-1 was highly expressed in HCC tumors, and associated with Sorafenib resistance[14]. In the present study, we specifically investigated CRIPTO-1 expression in a larger cohort of non-HCC cirrhosis, i.e. ALD and hepatitis B or C associated cirrhosis, to extend our previous findings. Interestingly, we found a statistically significant correlation between the amount of CRIPTO-1 protein staining and the laboratory MELD score, which illustrates that the CRIPTO-1 expression is related to the severity of the disease. Surprisingly, no correlation between the CRIPTO-1 and Sirius-red or

α-SMA staining was observed. This finding might be explained by the observation that these proteins are expressed by different cell types (hepatocytes vs stellate cells/myofibroblasts). Altogether, our data indicates that CRIPTO-1 expression could be a hepatocyte specific marker for the severity of liver fibrogenesis, similar to collagen and α-SMA for the stellate cells in a fibrotic liver.

Since blood samples are easier to obtain than liver biopsies, we also determined CRIPTO-1 levels in plasma samples of patients with ALD or viral hepatitis related end-stage liver cirrhosis to assess whether this might reflect the CRIPTO-1 accumulation in the liver. Most (69%) of the measured plasma samples showed elevated CRIPTO-1 levels prior to LT which decreased after the patients underwent LT. This observation is in line with recent findings of Zhang et al. who also observed enhanced CRIPTO-1 levels in serum of patients with HCV- and HBV-induced cirrhosis[36]. In concordance with the present study, they found undetectable CRIPTO-1 levels in some of the serum samples obtained from patients with cirrhosis. The reason for these undetectable CRIPTO-1 levels is unknown but in the present study it is unrelated to the disease stage (data not shown). In contrast to protein quantification of the liver tissue, CRIPTO-1 plasma levels did not correlate with the MELD score. This discrepancy might be related to the use of unpaired plasma-tissue samples, i.e. from different patients. A prospective study to evaluate individual liver-plasma CRIPTO-1 expression and correlation to MELD score needs to be performed to elucidate this potential relationship. Nevertheless, we observed decreased CRIPTO-1 plasma levels after LT in all samples from the patients that had detectable levels pre-LT. This finding strengthens our hypothesis that CRIPTO-1 is expressed during fibrogenesis since the elevated plasma levels decrease after removal of the fibrogenic source by the LT.

Our descriptive observations on the elevated CRIPTO-1 expression in the fibrogenic cascade does not provide information on the mechanism(s) which cause this increase. The liver is well-known for its regenerative capacity upon tissue injury[29-31]. Perhaps CRIPTO-1 is re-expressed as a response to cellular injury in order to survive the injuring stimuli and to promote the proliferation of hepatocytes. Research of Zhang et al. indeed showed that challenging HepG2 cells with harmful stimuli will lead to the upregulation of CRIPTO-1 which initiates apoptotic resistance and increased proliferation[15]. Altogether, this would suggest that CRIPTO-1 has an inducible function and can be activated by external liver injuring stimuli.

To conclude, CRIPTO-1 is known to be expressed only during embryogenesis and oncogenesis. We showed, however, that CRIPTO-1 is also expressed during fibrogenesis in livers of humans, mice and zebrafish embryos, indicative of a well preserved role for this growth factor protein in the pathology of hepatic fibrogenesis. Furthermore, CRIPTO-1 protein expression in liver tissue of humans was found to be correlated with the laboratory MELD score and elevated plasma CRIPTO-1 levels normalized after liver transplantation. Altogether the observations

from this study warrants further research to disentangle whether CRIPTO-1 has a functionally relevant role in liver fibrogenesis.

Acknowledgements

We thank the staffs of the central animal facility of the LUMC and the central zebrafish animal facility of the Gorleaus Laboratories for animal care and for maintaining the zebrafish population.

Disclosure of conflicts of interest

The authors confirm that there are no conflicts of interest.

References

1. Strizzi, L., Bianco, C., Normanno, N. *et al.* Cripto-1: a multifunctional modulator during embryogenesis and oncogenesis. *Oncogene* 2005; **24**: 5731-5741.
2. Strizzi, L., Margaryan, N. V., Gilgur, A. *et al.* The significance of a Cripto-1-positive subpopulation of human melanoma cells exhibiting stem cell-like characteristics. *Cell Cycle* 2013; **12**: 1450-1456.
3. Lo, R. C., Leung, C. O., Chan, K. K. *et al.* Cripto-1 contributes to stemness in hepatocellular carcinoma by stabilizing Dishevelled-3 and activating Wnt/beta-catenin pathway. *Cell Death Differ* 2018; **25**: 1426-1441.
4. Spike, Benjamin T., Kelber, Jonathan A., Booker, E. *et al.* CRIPTO/GRP78 signaling maintains fetal and adult mammary stem cells ex vivo. *Stem Cell Reports* 2014; **2**: 427-439.
5. Xu, C.-H., Sheng, Z.-H., Hu, H.-D. *et al.* Elevated expression of Cripto-1 correlates with poor prognosis in non-small cell lung cancer. *Tumor Biol.* 2014; **35**: 8673-8678.
6. Cocciadiferro, L., Miceli, V., Kang, K.-S. *et al.* Profiling cancer stem cells in androgen-responsive and refractory human prostate tumor cell lines. *Annals of the New York Academy of Sciences* 2009; **1155**: 257-262.
7. Terry, S., El-Sayed, I. Y., Destouches, D. *et al.* CRIPTO overexpression promotes mesenchymal differentiation in prostate carcinoma cells through parallel regulation of AKT and FGFR activities. *Oncotarget* 2015; **6**: 11994-12008.
8. D'Antonio, A., Losito, S., Pignata, S. *et al.* Transforming growth factor alpha, amphiregulin and cripto-1 are frequently expressed in advanced human ovarian carcinomas. *International journal of oncology* 2002; **21**: 941-948.
9. Fujii, K., Yasui, W., Kuniyasu, H. *et al.* Expression of CRIPTO in human gall bladder lesions *The Journal of Pathology* 1996; **180**: 166-168.
10. Giorgio, E., Liguoro, A., D'Orsi, L. *et al.* Cripto haploinsufficiency affects in vivo colon tumor development. *International journal of oncology* 2014; **45**: 31-40.
11. Sun, C., Sun, L., Jiang, K. *et al.* NANOG promotes liver cancer cell invasion by inducing epithelial–mesenchymal transition through NODAL/SMAD3 signaling pathway. *The International Journal of Biochemistry & Cell Biology* 2013; **45**: 1099-1108.
12. Tysnes, B. B., Satran, H. A., Mork, S. J. *et al.* Age-dependent association between protein expression of the embryonic stem cell marker Cripto-1 and survival of glioblastoma patients. *Translational Oncology* 2013; **6**: 732-741.
13. Wang, J. H., Wei, W., Xu, J. *et al.* Elevated expression of Cripto-1 correlates with poor prognosis in hepatocellular carcinoma. *Oncotarget* 2015; **6**: 35116-35128.
14. Karkampouna, S., van der Helm, D., Gray, P. C. *et al.* CRIPTO promotes an aggressive tumour phenotype and resistance to treatment in hepatocellular carcinoma. *J Pathol* 2018; **245**: 297-310.
15. Zhang, Y., Mi, X., Song, Z. *et al.* Cripto-1 promotes resistance to drug-induced apoptosis by activating the TAK-1/NF-kappaB/survivin signaling pathway. *Biomed Pharmacother* 2018; **104**: 729-737.
16. El–Serag, H. B. & Rudolph, K. L. Hepatocellular carcinoma: epidemiology and molecular carcinogenesis. *Gastroenterology* 2007; **132**: 2557-2576.

17. Friedman, S. L. Mechanisms of hepatic fibrogenesis. *Gastroenterology* 2008; **134**: 1655-1669.
18. Bataller, R. & Brenner, D. A. Liver fibrosis. *J Clin Invest* 2005; **115**: 209-218.
19. Lee, Y. A., Wallace, M. C. & Friedman, S. L. Pathobiology of Liver Fibrosis–A Translational Success Story (vol 64, pg 830, 2015). *Gut* 2015; **64**: 1337-1337.
20. Tunon, M. J., Alvarez, M., Culebras, J. M. *et al.* An overview of animal models for investigating the pathogenesis and therapeutic strategies in acute hepatic failure. *World J Gastroentero* 2009; **15**: 3086-3098.
21. van der Helm, D., Groenewoud, A., de Jonge-Muller, E. S. M. *et al.* Mesenchymal stromal cells prevent progression of liver fibrosis in a novel zebrafish embryo model. *Sci Rep* 2018; **8**: 16005.
22. Byass, P. The global burden of liver disease: a challenge for methods and for public health. *Bmc Med* 2014; **12**:
23. Liver, E. A. S. EASL Recommendations on Treatment of Hepatitis C 2016. *J Hepatol* 2017; **66**: 153-194.
24. Mathurin, P., Hadengue, A., Bataller, R. *et al.* EASL Clinical Practical Guidelines: Management of Alcoholic Liver Disease. *J Hepatol* 2012; **57**: 399-420.
25. Lee, Y. A. & Friedman, S. L. Reversal, maintenance or progression: What happens to the liver after a virologic cure of hepatitis C? *Antivir Res* 2014; **107**: 23-30.
26. Angaswamy, N., Tiriveedhi, V., Sarma, N. J. *et al.* Interplay between immune responses to HLA and non-HLA self-antigens in allograft rejection. *Hum Immunol* 2013; **74**: 1478-1485.
27. Lucidi, V., Gustot, T., Moreno, C. *et al.* Liver transplantation in the context of organ shortage: toward extension and restriction of indications considering recent clinical data and ethical framework. *Curr Opin Crit Care* 2015; **21**: 163-170.
28. Mesens, N., Crawford, A. D., Menke, A. *et al.* Are zebrafish larvae suitable for assessing the hepatotoxicity potential of drug candidates? *J Appl Toxicol* 2015; **35**: 1017-1029.
29. Fausto, N. & Campbell, J. S. The role of hepatocytes and oval cells in liver regeneration and repopulation. *Mech Dev* 2003; **120**: 117-130.
30. Fausto, N., Campbell, J. S. & Riehle, K. J. Liver regeneration. *Hepatology* 2006; **43**: S45-53.
31. Gilgenkrantz, H. & Collin de l'Hortet, A. Understanding Liver Regeneration: From Mechanisms to Regenerative Medicine. *Am J Pathol* 2018; **188**: 1316-1327.
32. van der Helm, D., Barnhoorn, M. C., de Jonge-Muller, E. S. M. *et al.* Local but not systemic administration of mesenchymal stromal cells ameliorates fibrogenesis in regenerating livers. *J Cell Mol Med* 2019;
33. Her, G. M., Chiang, C. C., Chen, W. Y. *et al.* In vivo studies of liver-type fatty acid binding protein (L-FABP) gene expression in liver of transgenic zebrafish (Danio rerio). *FEBS Lett* 2003; **538**: 125-133.
34. Sebastiani, G., Castera, L., Halfon, P. *et al.* The impact of liver disease aetiology and the stages of hepatic fibrosis on the performance of non-invasive fibrosis biomarkers: an international study of 2411 cases. *Aliment Pharmacol Ther* 2011; **34**: 1202-1216.
35. Afify, S. M., Tabll, A., Nawara, H. M. *et al.* Five Fibrosis Biomarkers Together with Serum Ferritin Level to Diagnose Liver Fibrosis and Cirrhosis. *Clin Lab* 2018; **64**: 1685-1693.

36. Zhang, Y., Xu, H., Chi, X. *et al.* High level of serum Cripto-1 in hepatocellular carcinoma, especially with hepatitis B virus infection. *Medicine (Baltimore)* 2018; **97**: e11781.

Supplementary files

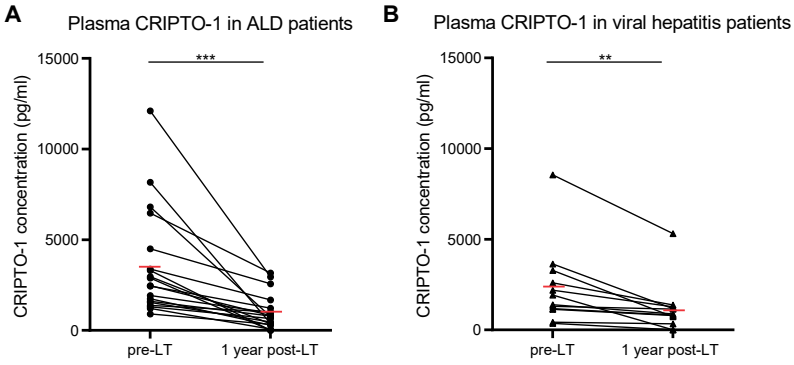

Supplemental figure 1. CRIPTO-1 levels in aetiological sub-cohorts. CRIPTO-1 levels in pre- and post-LT paired plasma samples of patients suffering from (A) ALD (N=19) or (B) viral (N=12) induced liver cirrhosis. Mean group levels are indicated by a red line. **p≤0.01 ***p≤0.001

Supplemental table 1: Primer sequences

Gene	Forward	Reversed
Human		
α-smooth muscle actin	TTGCCTGATGGGCAAGTGAT	GTGGTTTCATGGATGCCAGC
Collagen-1α1	GGAACTTGGGGCAAGACAGT	GAGGGAACCAGATTGGGGTG
CRIPTO-1	CACGATGTGCGCAAAGAGAA	TGACCGTGCCAGCATTTACA
β-actin	AATGTCGCGGAGGACTTTGATTGC	GGATGGCAAGGGACTTCCTGTAAA
Mouse		
α-smooth muscle actin	GTCCCAGACATCAGGGAGTAA	TCGGATACTTCAGCGTCAGGA
Collagen-1α1	GTGGAAACCCGAGCCCTGCC	TCCCTTGGGTCCCTCGACGC
CRIPTO-1	CGCCAGCTAGCATAAAAGTG	CCCAAGAAGTGTTCCCTGTG
β-actin	GGGGTGTTGAAGGTCTCAAA	AGAAAATCTGGCACCCC
Zebrafish		
Acta-2	TTGTGCTGGACTCTGGTGAT	GGCCAAGTCCAAACGCATAA
Collagen-1α1	CTTTTGCTCACAGGGCCTTT	AAGACTGCATGCATCACAGC
CRIPTO-1	GGCTCCCTCAGAACACTGTC	CGTTCAACAGGGGAGATCAT
Ribosomal protection protein	CTGAACATCTCGCCCTTCTC	TAGCCGATCTGCAGACACAC